

ACOUSTIC EMISSION FROM RUST IN STRESS CORROSION CRACKING

**Hideo Cho, Aoyama Gakuin University, Sagamihara Kanagawa, JAPAN
Prof. Mikio Takemoto, Aoyama Gakuin University, Sagamihara Kanagawa, JAPAN**

ABSTRACT

Petrochemical and nuclear plants are located in coastal area in Japan and tend to suffer SCC in heat-affected zone (HAZ) by sea-born salt. Stress corrosion cracking on the outer surface (external SCC or ESCC) of aged storage tanks and pipelines is becoming serious problem. AE detection of ESCC of insulated equipments is expected, however, AE can hardly monitor the occurrence of chloride-induced transgranular type SCC (TG-SCC) since no strong AEs can be produced by TG-SCC. SCC progression can be monitored by acoustic emission if the fracture of rust in cracks produces strong AEs. We studied characteristics of Lamb wave AEs during rust growth in SCC of butt-welded AISI 304. Both pipe and shells were studied as a function of wall temperature from 298 K to 253 K.

Key words: External stress corrosion cracking (ESCC), chloride SCC, Rust fracture, volumetric expansion, Lamb wave AE, Cylinder wave AE

INTRODUCTION

Among various types of stress corrosion cracking (SCC), SCC of austenitic stainless steel by chloride anions is the most serious problem in chemical, petro-chemical, food and nuclear power plants. SCCs on the outer surface of equipment and tubing, called as the External SCC (ESCC) is becoming important problems for aged plants. Also health monitoring of new storage vessels of spent nuclear fuel for over 40 years is another important technology.

Chemical causes of ESCC of austenitic stainless steel are chloride ions induced by sea salts and in the insulations such as hard urethan rubber, and sometimes vinyl-chloride adhesive tapes in nuclear power plants. As the most chemical and petro-chemical plants in Japan are located in the coastal area, thermal insulations are contaminated by sea-born salts and unacceptable chloride level at present. ESCC tends to occur at equipments whose surface temperature are below approximately 340K and is generally transgranular type. Wet insulation offers the place in which chloride and

sometimes fluoride ions concentrate. Takemoto first reported the harmfulness of fluoride ions in ESCCs [1]. Fluoride ions appears to come from wet welding fume and detrimental to the sensitized stainless steels below 340 K.

Eye-inspection of ESCC, especially those under the thermal insulations, is time- and cost-consuming problems. This type of inspection is impossible in nuclear-related equipments. Some plant owners have recently utilized AE for monitoring the chloride ESCC, but could not detect the AEs. Okada [2] reported no AE from chloride-SCC of AISI304 steel, possibly due to the active path corrosion (APC) mechanism [2]. We recently confirmed that the transgranular type chloride SCC of AISI 304 steel does not produce AEs while Intergranular type SCC (IG-SCC) of 304 steel does produce AEs [3]. For the ESCCs of process equipments, we observe much rusting around the SCCs.

Rusts growth in fine crevice or cracks, as well those on free surface, produces strong AEs due to their volumetric expansion during growth [4]. Hard rust in crevice sometimes produces new tensile stresses and resulted in complicated SCC propagation, as will be discussed later. This suggests that we can monitor the progression of SCC and ESCC by detecting the secondary AEs produced by rust fracture in the fine crevice.

We first studied the fracture dynamics of natural rust produced on carbon steel exposed to out-door weathering for 500 days by AE source inversion. Next we monitored AEs from rusting in SCC. Three types of experiment were conducted. One is AE monitoring from heating-and-cooling operation of a butt-weld pipe with SCC painted by chloride solution. Second is the AE monitoring during wet-and-dry operation of weld shell with SCC. Third is the AE monitoring from a clad steel plate (clad 304 steel on carbon steel) which suffered severe SCCs during 12 years service in salt-producing plants.

FRACTURE DYNAMICS OF NATURAL RUST BY AE SOURCE INVERSION

AEs from natural rust fracture is important not only for SCC monitoring of process equipment but also for corrosion monitoring of steel structures exposed to weathering. We first studied fracture dynamics of natural rust by waveform simulation of the Lamb wave AEs. We exposed coupon-shaped carbon steel plates (40mm wide-200 mm long and 1mm thick) to the out-door weathering for 500 days and prepared steel plates with natural rust of approximately 0.4 mm thickness. Reduction of wall thickness of the plate is approximately 0.1mm. Natural rust is composed of γ -FeOOH (lepidocrysite), Fe_3O_4 (magnetite, black rust) and Fe_2O_3 (hematite, red rust).

Using four AE sensors (PAC, PICO) mounted on the surface of the plate as shown in Fig.1, we monitored Lamb wave AEs during four point bending. Figure 2 shows cumulative AE counts as a function of surface strain. Strong AEs, as shown in Fig. 3, were monitored from small surface tensile strains. Waveforms matching of So-packets revealed crack opening of $1.4 \times 10^{-14} \text{ m}^3$ at 0.7 μs . It is

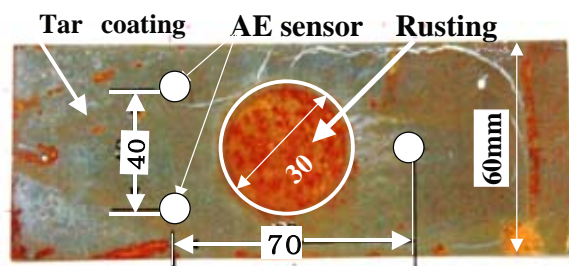


Fig.1 Atmospheric rust produced on SPC steel plate exposed to outdoor weathering for 500 days

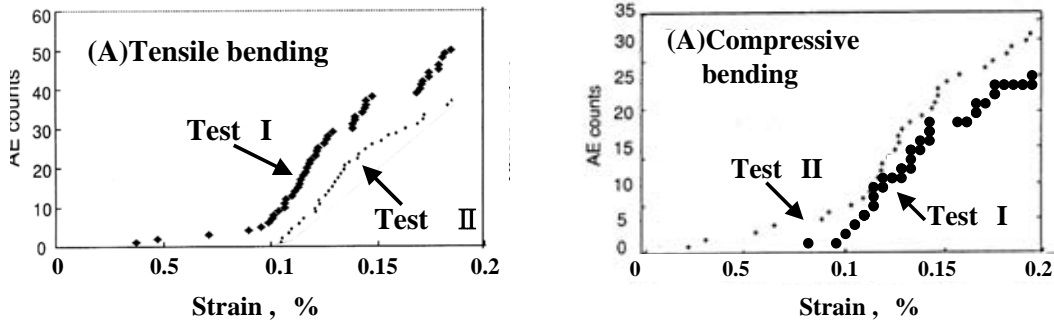


Fig.2 Cumulative AE counts vs. substrate strain

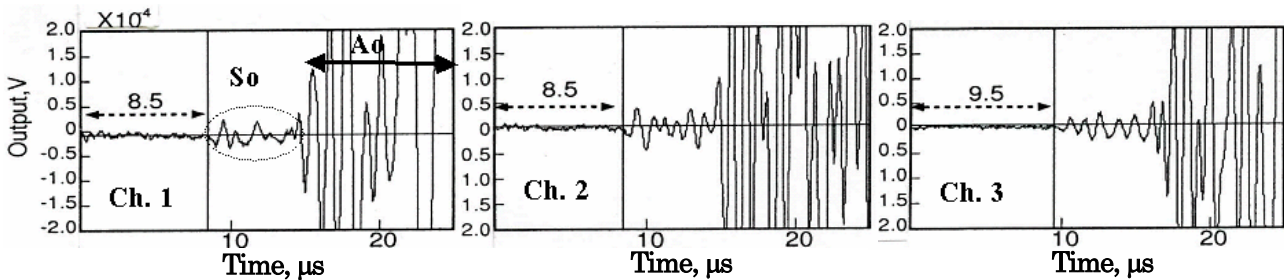


Fig.3 Lamb wave AEs due to Mode-I fracture of the rust produced by atmospheric corrosion.

noted that the source rise time is almost the same those of delayed microcracks [5], but the crack volume is thousands times larger those of the delayed fracture. As shown in Fig. 4, Mode-I fracture of the surface rust with an opening vector in the axial direction was apparent, and produces strong AE. We could also detect strong AEs from growing natural rust of steel plate exposed to out-door weathering [6]. As the rust growth takes times, we can not detect the initiation of corrosion and SCC by AE, but monitor the progression of them by AE.

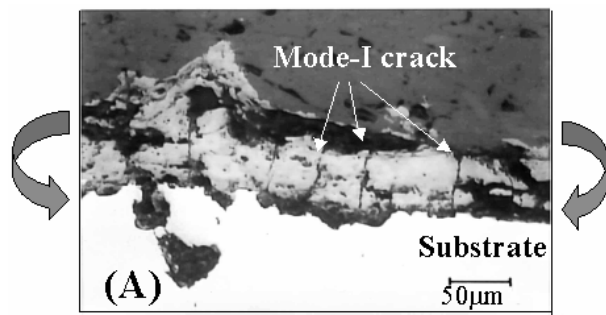


Fig.4 Transverse structure of the atmospheric rusts after tensile bending test

AEs FROM RUST FRACTURES IN ESCC OF BUTT-WELD 304 PIPE

In order to study the AEs from rust growth in SCC, we first produced ESCC on the outer surface of a butt-weld 304 steel pipe of 3/4 inch diameter by immersion the pipe vertically in a boiling 35mass % magnesium chloride solution for 410 h. Circumferential SCC of 25 mm long was produced by residual tensile stresses in HAZ as shown in Fig.5. We also observed severe red rust over the splash zone of the pipe along axial scratch. This rust was later found to be produced by axial SCC caused by scratch-induced residual stresses. It is noted that the 304 steel does not suffer any rust over the polished free surface in the chloride solution, but does suffer severe rusting along scratch and crack by the wet-and-dry operation.

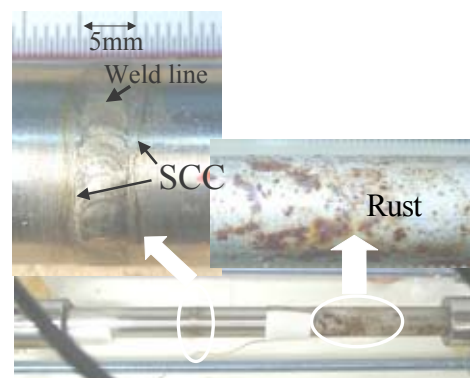


Fig.5 SCC damaged butt-weld 304 pipe

Next we monitored cylinder wave AEs of this pipe during heating-cooling operation in air. Two monitoring methods were utilized as shown in Fig.6. Two AE sensors of PAC R3I with a head-amplifier were mounted on the pipe edges, and two PICO sensors on the pipe surface at 50 mm (left) and 55 mm (right) from the weld line. It is noted that the right R3I sensor was 150 mm from the weld line and the left one from 70 mm. Outputs of these sensors were amplified by 40 dB and stored in a computer simultaneously. Pipe surface around HAZ was painted by 35 mass % MgCl₂ solution once and heated by an infrared lamp to 333 K for 42.6 ks and then cooled. Figure 7 shows the cumulative AE counts by R3I sensors during cooling (OFF) and heating (ON) cycle. Here, solid line of “near Ch.1” designates the AEs whose sources were close to the channel 1 sensor or the weld line. Broken line indicates AEs from the rust on the right surface close to the channel 2 sensor. We observed several hundreds of AE events at later period of heating. Figure 8 presents an example of cylinder wave AEs. First arrival packet of waveforms by R3I sensors represents the L(0,1) or breathing mode. Theoretical group velocity of L(0,1) is calculated as 4800 m/s and agrees well with the experimental velocity of 4700 m/s. Source location in the axial direction of the pipe is shown in Fig. 9. Sources are located near the SCC and the right rust on the surface. We next cut the pipe at b-b’ line and examined the transverse structure. As shown in Fig. 10, we found SCC under the rust (a). The SCC was filled with rust (b). This suggests that the AE events shown by the broken line (near Ch.2) of Fig. 6 are from the rust on the pipe surface as well as the rust fractures in the SCC. It noted that the free surface of the pipe are free from any rust even in the SCC test and following heating-cooling operation, but the SCC accelerates significantly the rust formation.

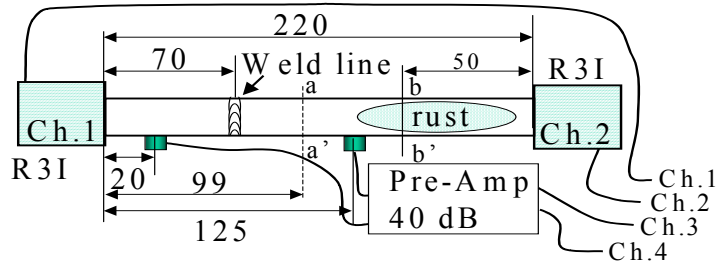


Fig.6 Experimental setup for butt-weld 304 pipe sample.

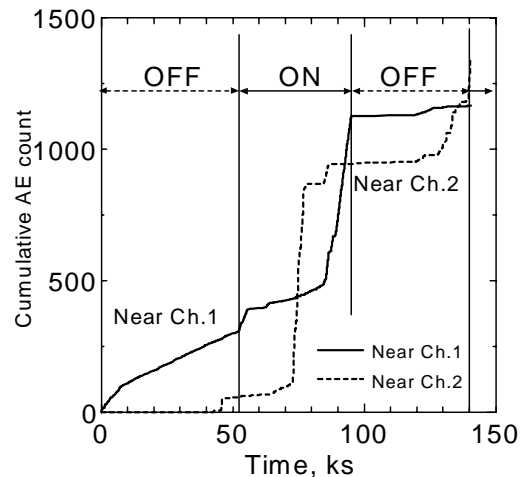


Fig.7 Cumulative AE count vs. time

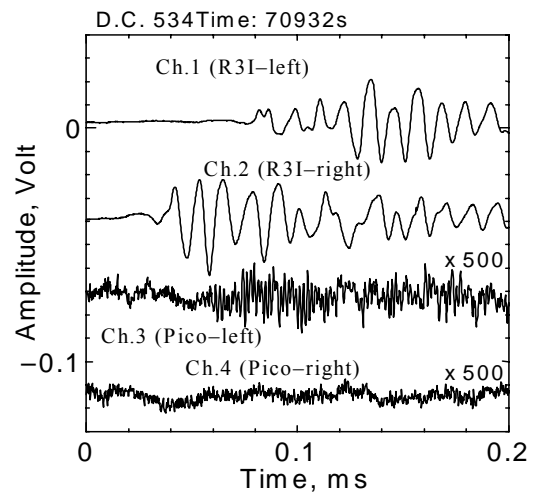


Fig.8 Typical AE as cylinder waves from rust cracking.



Fig.9 Estimated AE source location on the pipe.

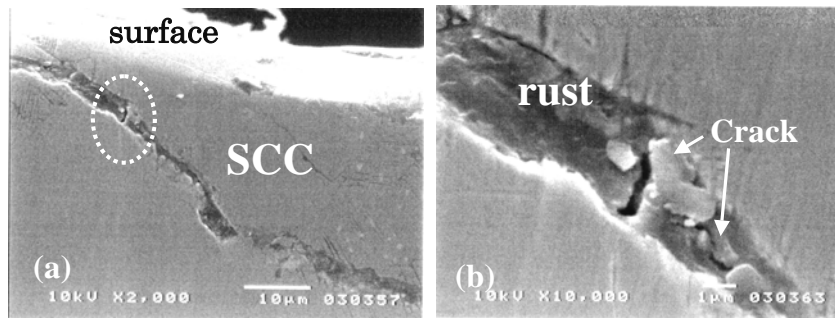


Fig. 10 SCC in the cross-section of pipe (a) and crack in the rust in SCC (b)

As the AE amplitude of the PICO sensor (Fig. 8) was weak, we next monitored AEs using M201 sensor (JT Toshi. Co. with a head-amplifier). Two M201 sensors were mounted on the pipe surface. One sensor was on the left surface at 15 mm and another on the right surface at 47 mm from the weld line. Now the left R3I sensor is at 28 mm from the weld line and the right one from 71 mm. Figure 11 shows an example of Lamb wave AEs by R3I and M201 sensors. Amplitudes of AEs from rust fracture are weak due to small crack volumes than that of natural rust formed on the free surface. We, however, can detect AEs from the rust in SCC.

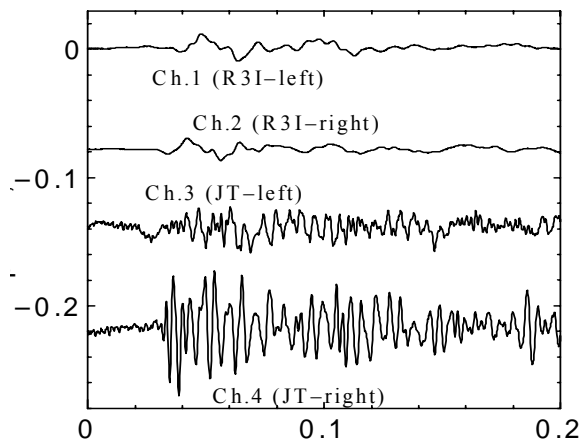


Fig.11 Detected AE waveform by another small sensor (JT-toshi)

AEs FROM RUST IN ESCC OF WELD 304 THIN WALL SHELL

AEs from rust growth in SCC of thin wall shell were monitored for approximately 16 days. SCC was priory induced by 373 K MgCl₂ solution as shown in Fig. 12, more than seven branched SCCs were produced across the weld line after 30 days exposure. Lamb wave AEs were monitored by four R6I sensors (gain 40 dB) mounted in the cylinder jigs as shown in Fig. 12. Shell inside was heated by an infrared lamp for 8 hours every day. Outer surface of the SCC was subjected to the water mist spray for 0.5 h and dried for 3.5 hr cycle. Fig. 13 shows typical AE waves. Amplitudes of AE were in the range of 80 to 100 mVp-p after 40 dB amplification. As So-packets were clearly detected by only Ch.4 sensor, we located AE sources from the arrival times of the first A_o mode wave. Figure 14 shows AE source location map.

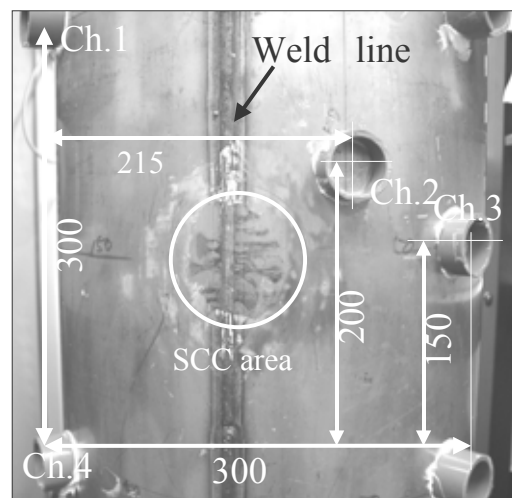


Fig.12 Thin wall hollow cylinder with SCC damage and sensor location.

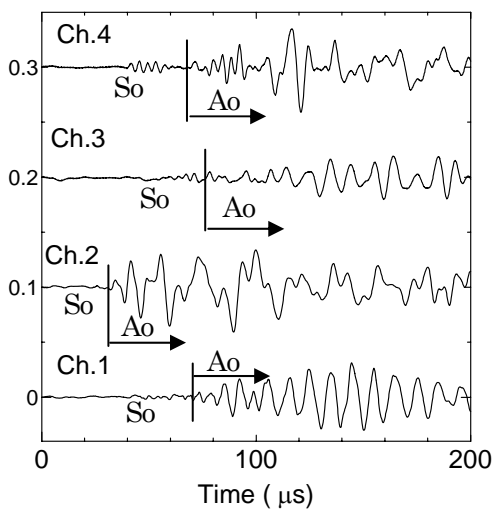


Fig.13 Typical AE waves as lamb wave from rust fracture.

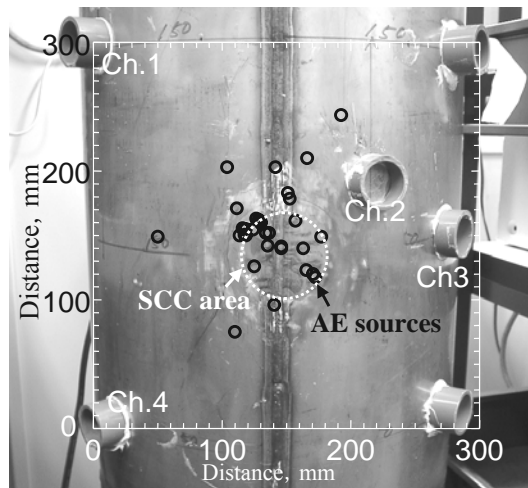


Fig.14 Estimated AE source location of thin wall hollow cylinder sample.

AE sources were located near the SCC area. Fig.15 shows cumulative AE counts during test. Masked areas designate the heating periods. Surface temperature reached 353 K by heating. AE generation rate gradually increased with time, possibly due to rust growth. After 900 ks (Fig. 16), many AEs were generated during mist spraying and temperature down. This suggests that AEs are generated by rust fracture due to not only the rust growth but also the stresses induced by crack wall.

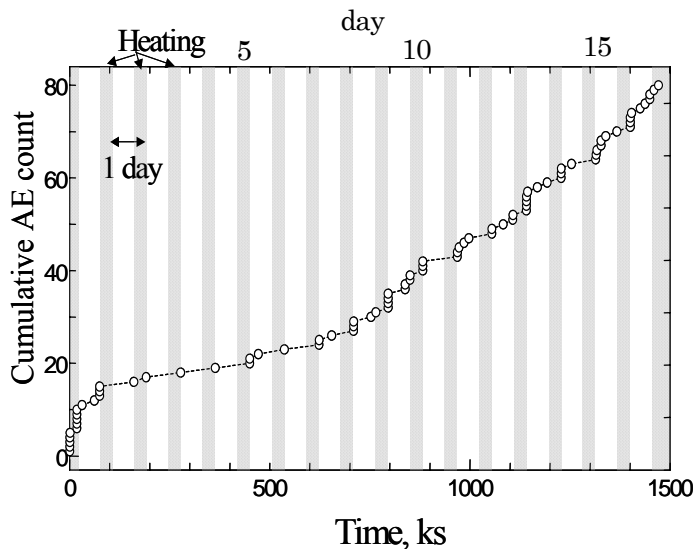


Fig.15 Cumulative AE count and heating cycle history during AE monitoring.

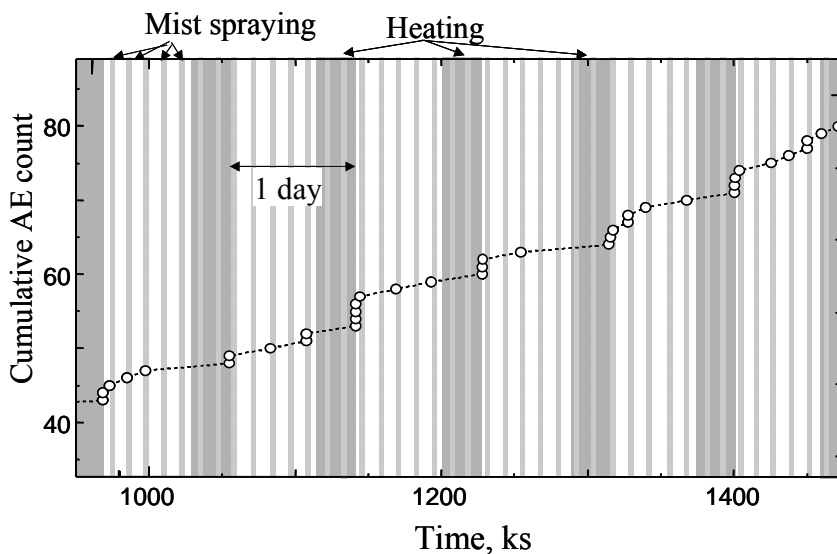


Fig.16 Expanded Cumulative AE count history after 900ks

AE FROM RUST IN SCC ON CLAD STAINLESS STEEL PLATE TAKEN FROM SALT PRODUCING PLANT

The sample tested is a clad stainless steel taken from an evaporator in salt producing plant. Clad stainless steel suffered severe SCC in HAZ after 12 years service. Stainless layer (2 mm thick) exfoliated partially from the substrate carbon steel (6 mm thick) as shown in Fig. 17. SCC reached the substrate carbon steel and is filled with dense rust (magnetite) produced by severe galvanic corrosion (Fig. 18). Dense and hard rust ($H_v=280$) produces tensile stresses to cause new lateral SCCs and accelerates the exfoliation of clad stainless layer. This is a sample of internal SCC, but expected to produce strong AEs by further rusting in the cracks. We monitored AEs using two R6I sensors mounted on the clad stainless steel surface. Rusting was produced by painted 35mass % $MgCl_2$ solution in an O-ring set over the weld line. The sample was heated to 308 K to 318 K by a lamp. Figure 19 shows event count vs. exposure time. AE event increased after 50 ks exposure, and increased with time. First 50 ks is considered to be the time during which new rust is produced. Typical Lamb wave AEs are shown in Fig. 20. Sources of 20 events are located in the O-ring.

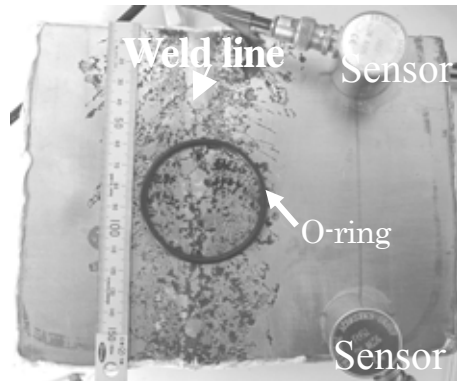


Fig.17 Surface appearance of SCC in SUS304 clad steel taken from circulation pipe of salt-producing plant.

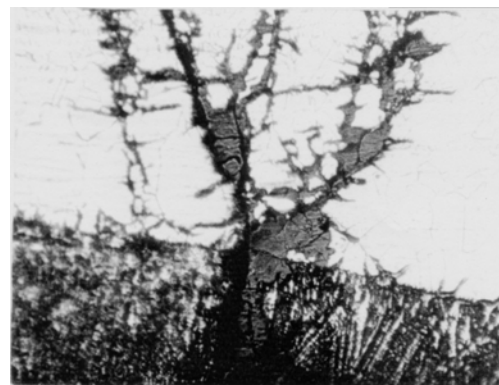


Fig. 18 Transverse SCC through clad SUS304 with hard rust in it and surface parallel cracks produced by wedge effect.

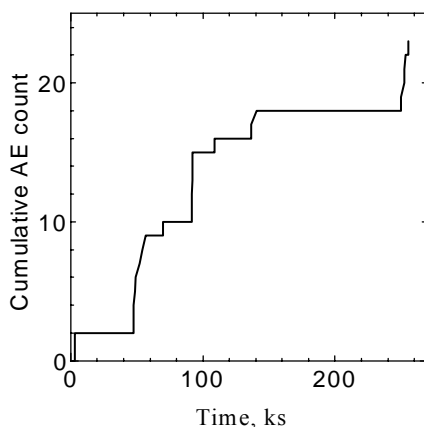


Fig. 19 cumulative AE count vs. time

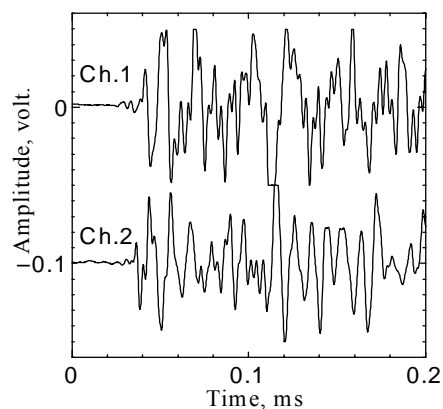


Fig. 20 typical AE waveform as Lamb waves

CONCLUSION

With the aim of remote monitoring of SCC progression by AE, we first studied fracture dynamics of natural rust on steel plate by the waveform matching of So-mode Lamb wave AEs. Source rise times of natural rust fracture are almost the same those of micro-cracks in delayed fracture of high tension steel, but the crack volumes are thousands times larger those of the delayed fracture. Next, we monitored AEs from the rust fracture in SCC of butt-weld and clad stainless steel. We detected a number of AEs during heating-cooling and wet-dry operation of SCC. These AEs are considered to be produced by rust fracture due to the volumetric expansion of the rust and due to the fracture forces from the crack wall by heat cycle. Though the amplitude of AE was not so strong due to small crack volume, we can monitor the progression of SCC by acoustic emission technique.

Literature cited

- [1] M.Takemoto, External Stress Corrosion Cracking (ESCC) of Austenitic Stainless Steel, Materials Performance, 24-6,(1985)pp.26-32
- [2] H.Okada, Y.Yukawa and H.Tamura, Corrosion, 30,253(1974)
- [3] S.Fujimoto, M.Takemoto and K.Ono, J, Acoustic Emission, 19,63(2999)
- [4] M.Takemoto, T.Sogabe,K.Matsuura and K.Ono, Progress in Acoustic Emission XI, p45(2002)
- [5]M.Takemoto, Y.Hayashi and M.Takemoto, J. Jpn. Soc. Nondestructive Inspection (in Japanese),43,637(1994)
- [6]T.Sogabe and M.Takemoto, J. Jpn. Soc. Nondestructive Inspection (in Japanese), 53,35(2004)